Clay Minerals, (2013) **48**, 295–308

Dissolution experiments of Na- and Ca-montmorillonite in groundwater simulants under anaerobic conditions

E. MYLLYKYLÄ[1,*], M. TANHUA-TYRKKÖ[1], A. BOUCHET[2] AND M. TILJANDER[3]

[1]*VTT Technical Research Centre of Finland. P.O.Box 1000, FI-02044 VTT, Finland,* [2]*Etudes Recherches Matériaux ERM, Centre Régional d'Innovation du Biopôle, 4 rue Carol Heitz, 86000 Poitiers, France, and* [3]*Geological Survey of Finland, P.O. Box 96, FI-02151 Espoo, Finland*

(*Received 4 December 2012; revised 7 March 2013; Editor: John Adams*)

ABSTRACT: The effects of simulant groundwater composition, pH and temperature on the dissolution and alteration of Na- and Ca-montmorillonite have been studied. Prior to the experiments, Wyoming type Na-montmorillonite, Swy-2, was purified to decrease the amount of accessory minerals. For Ca-montmorillonite experiments, the interlayer cation Na^+ of purified Swy-2 was exchanged with Ca^{2+}. The batch experiments were conducted with the purified montmorillonites in simulated fresh and saline waters at 25ºC and 60ºC under anaerobic conditions in an Ar atmosphere. The concentrations of Si, Al, Fe and Mg were analysed from ultra-filtered solution samples with High Resolution Inductively Coupled Plasma Mass Spectrometry (HR-ICP-MS) as a function of dissolution time. The pH evolution was also measured. The solid smectite phases were analysed with X-ray Diffraction (XRD) and Scanning Electron Microscopy (SEM). XRD analyses indicated that the nature of the smectite mineral did not change over 140 days. However, the experimental conditions, more or less, modified the structure (e.g. the layer stacking of montmorilllonite; the partial dissolution of the smectite), which cannot be detected by XRD but was evidenced by chemical data, and can be considered as a possible contributor to the stacking faults of the montmorillonite. The log rates (mol g^{-1} s^{-1}), based on the dissolved amount of Si, varied between −10.64 and −12.13 depending on the experimental conditions.

KEYWORDS: dissolution, montmorillonite, groundwater, anaerobic conditions, bentonite buffer, alteration.

In many nuclear waste disposal concepts bentonite is planned to be used as a sealing material. The buffer properties of bentonite are largely based on the properties of its main mineral, montmorillonite. Therefore knowledge of the behaviour of montmorillonite in various environments is necessary in order to understand those processes in which bentonite is involved.

Some dissolution studies of smectite clays have been conducted under aerobic conditions over the past 50 years. Good overviews of those studies are presented in e.g. Rozalen *et al.* (2008, 2009) and Marty *et al.* (2011). In general, montmorillonite, like many other minerals, e.g. biotite (Malmström *et al.*, 1996) and quartz (Brady & Walther, 1990; Knauss & Wolery, 1987), dissolves as a function of ionic strength, ΔG and temperature (Lasaga, 1998). Generally, the dissolution rates of smectite decrease as pH increases in the acidic domain, reaching a minimum near neutral pH, and increase again in the basic domain with increasing pH. The ionic strength of the solution can also have an effect on solubility (Zysset & Schindler, 1996). The reactive surface area, catalysing/inhibiting species and the saturation

* E-mail: emmi.myllykyla@vtt.fi
DOI: 10.1180/claymin.2013.048.2.11

state of the solution may also contribute to the dissolution kinetics. In realistic cases, considering the final disposal system, the flow rate of the liquid phase and the degree of compaction of the clay may have a relevant role in the dissolution kinetics.

The aim of this study was to gain a better understanding of the behaviour of montmorillonite in contact with groundwater. To the knowledge of the writers there are no published studies of the dissolution of montmorillonite under anaerobic conditions. Instead of using natural groundwater we used saline and fresh simplified waters based on reference groundwaters chosen for the Olkiluoto site in Finland. Saline water simulant represents the prevailing groundwater conditions at disposal level (−420 m), but has elevated pH, which may occur in the after closure conditions in the disposal facility. Fresh water simulates the presumed disposal conditions caused by glacial melt waters in the far future. Special attention was paid to the dissolution rates and alteration of the dissolving smectite clay.

EXPERIMENTAL

Purification and ion exchange of Swy-2

Prior to the experiments, the solid material Wyoming type Na-montmorillonite, The Clay Mineral Society's (CMS) Swy-2 [$(Ca_{0.06}Na_{0.16}K_{0.025})(Al_{1.51}Fe_{0.205}Mn_{0.005}Mg_{0.28}Ti_{0.01})(Si_{3.99}Al_{0.01})O_{10}(OH)_2$] was first purified to decrease the amount of quartz and other accessory minerals (Chipera & Bish, 2001). The bentonite purification procedure was based on the work of Tournassat *et al.* (2004), Ammann (2003), and Baeyens & Bradbury (1995). The eight-step procedure is described in more detail in Myllykylä *et al.* (2011). After purification, the montmorillonite was predried in a heating chamber at 60ºC for approximately one day and then the moist montmorillonite was freeze dried for three days and thereafter ground with a pestle in a percussion mortar.

In order to produce Ca-montmorillonite for the experiments, 85 g of purified Na-montmorillonite was treated three times with 2 l of 1 M $CaCl_2$ solution; the Na-montmorillonite was washed by shaking with $CaCl_2$ overnight, then the phases were separated by centrifugation and the solution was discharged. Thereafter, the Ca-montmorillonite obtained was fractioned by washing it several times with deionized water in order to remove excess salt. After each washing step, the clay suspension was collected. Next, all the collected clay slurry was packed into a dialysis membrane and shaken in a 10 l bath of deionized water at room temperature. The dialysis was continued by replacing the water in the bath until a conductivity value of 0.01 mS/cm was reached, which took seven days. After dialysis, the Ca-montmorillonite was predried, freeze-dried and ground similarly to the Na-montmorillonite.

Batch experiments

Before starting the experiments, the Na- and Ca-montmorillonites were kept in containers sealed with parafilm under Ar atmosphere in a glove-box (O_2 in gas <10 ppm, T = 25±1.5ºC) for several days in order to minimize the amount of oxygen in the clays. The first step in preparing the two groundwater simulants, the fresh (I = 0.005 M, pH 8) and saline (I = 0.1 M, pH 11) waters, was to add $CaCl_2$ and NaCl to MilliQ-water and purge the solutions overnight in closed bottles with Ar prior to transferring them into the glove box. Purging of the waters was continued in the glove box for a few more hours. To finalize the water compositions, KCl, Na_2SO_4 and NaBr, were added in the glove-box as small aliquots from two stock solutions (KCl-Na_2SO_4 or KCl-NaBr). The stock solutions had also been prepared in the laboratory and purged with Ar and then kept in the glove-box. The compositions of the fresh and saline waters are given in Table 1. To achieve the desired pH value, NaOH was added to the waters and the waters were allowed to equilibrate for a few days at 25ºC. The pH values of the waters in 60ºC were calculated with the geochemical code EQ3NR (Wolery, 1992). In 60ºC, the pH of fresh water is 7.1 and the pH of saline water 10.1.

For the batch tests, 0.5 g of montmorillonite powder was weighed into 250 ml centrifuge bottles (Beckmann) to which either 250 ml of fresh or saline simulated groundwater was added. The solid-to-solution ratio was 2 g /l. Duplicate samples were prepared for each test. The tests were conducted in anaerobic conditions at 25 and 60ºC. Taking into account two different water simulants, two temperatures, and duplicate samples, the experiments had 8 tests for both Na- and Ca-montmorillonite.

In addition, parallel tests for each batch experiment were performed. In these tests, the solution phase was renewed twice during the

https://doi.org/10.1180/claymin.2013.048.2.11 Published online by Cambridge University Press

TABLE 1. Compositions of the fresh and saline groundwater simulants used in the experiments.

Fresh water, I = 0.005 M, pH 8		Saline water, I = 0.1 M, pH 11	
Salts used for preparation	Amount (mg/l)	Salts used for preparation	Amount (mg/l)
$CaCl_2x2H_2O$	52.4	$CaCl_2x2H_2O$	3000.5
NaCl	156.2	NaCl	2262.5
KCl	20.7	KCl	12.5
Na_2SO_4	39.4	NaBr	24.4

experiment to study the enhanced alteration of montmorillonite in the XRD analyses and to compare the results with those obtained in the batch tests without replacement of solution.

Figure 1 describes the experimental set-up of the tests conducted under anaerobic conditions in the glove box (25ºC) and those inside a steel container in a heating chamber (60ºC).

The samplings were performed at 2- to 5-day intervals in the beginning of the tests. After 20 days the sampling intervals were extended to 2 weeks. The final samples from the Na experiments were taken on the 114th day and from the Ca-montmorillonite experiments on the 137th day. Prior to sampling of the batch test, the suspension was agitated in order to maintain the solid/solution ratio as constant as possible. 8 ml samples for elemental analyses (Si, Mg, Al and Fe) were taken and ultrafiltered with centrifugal devices (Pall, Macrosep 10K Omega (~1 nm)) in a centrifuge (6430 rpm, 3 h, BeckmanCoulter Avanti J-26 XPI). The filtered samples were acidified with nitric acid (65% supra pure nitric acid, Merck) and stored in a refrigerator for further sample preparation and analysis. The pH was measured, directly from the test vessels, with an Orion ROSS combination electrode under Ar atmosphere in the glove-box. In the 60ºC tests, the temperature of the solution was about 40ºC while pH was measured.

Analyses

A scanning electron microscope (SEM) was used to characterize the mineralogical changes in the initial Na-montmorillonite (Swy-2) both before and after the purification. SEM-Feature analyses were performed in high-vacuum and with carbon-coated samples using SEM (JEOL JSM 5900 LV with EDS

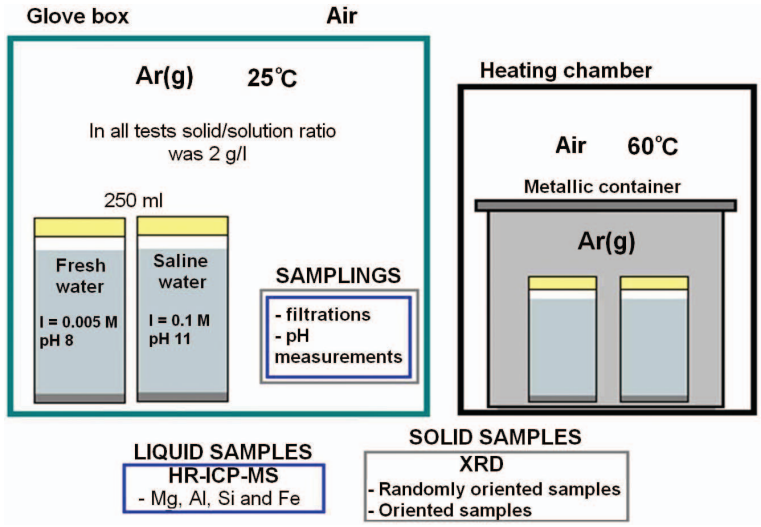

FIG. 1. Experimental setup of batch experiments conducted under anaerobic conditions.

https://doi.org/10.1180/claymin.2013.048.2.11 Published online by Cambridge University Press

spectrometer). Sample preparates were prepared by impregnating samples to epoxy (15:2, EpoFix Resin: EpoFix hardener). The Swy-2 sample was prepared from powdered material and the purified Swy-2 sample from freeze-dried material, which displayed a visible layer structure. The surface of the hardened samples was polished with fine sandpaper.

Samples of the original Swy-2, the purified Swy-2 Na-montmorillonite, the purified Swy-2 exchanged to Ca form, 8 solid samples from the batch experiment, and 8 samples from batch experiments with solution renewal, were prepared and analysed with X-ray diffraction (XRD). Prior to the sample preparation, the solids from Ca montmorillonite tests were washed three times with 70% ethanol in the Ar glove-box. The samples for XRD analysis were prepared by first drying the wet material in an oven (40ºC) for one day. The dry material was then crushed in an agate mortar and sieved (<80 μm) for recording of the randomly oriented powder pattern (determination of mineral components present in amounts greater than their own detection limit). Because of the small amount of sample, a special sample holder adapted for small quantities of material was used. Two patterns were recorded with oriented samples prepared in order to identify the clay minerals. The first record was made with the air-dried sample and the second pattern was recorded after ethylene glycol solvation of the oriented sample. The oriented aggregate samples were prepared by adding distilled water to the wet clay suspension which was then treated with ultrasound (3 min with 44%, Biblock Scientific vibracell 75043) to disintegrate the particles. Next, a few drops of sodium hexametaphosphate was added to reduce aggregation. A drop of the suspension was pipetted onto a glass slide and dried in air. While this type of preparation of a sample is unsuitable for quantitative analysis, it does not pose any problem for qualitative analysis (Reynolds, 1980; Moore & Reynolds 1989).

X-ray diffraction patterns were performed by ERM (Etudes Recherches Matériaux, Poitiers; France). A Bruker D8 Advance A25 diffractometer (Cu-*K*α radiation) equipped with a LynxEye detector was used. The analytical parameters were 40 kV and 40 mA. The mathematical treatment of data was performed with the Eva (Bruker) software. In the presence of mixed-layered phyllosilicates, the patterns were compared with the data computed by Reynolds (1980, 1985) and Moore & Reynolds (1989).

ICP-MS analyses of Si, Fe, Al and Mg concentrations in the ultrafiltrated solution samples were performed with Thermo Scientific's Element 2 device, equipped with a double focusing sector field magnet. The ICP was operated at medium resolution (M/ΔM = 4000). Standard solutions were prepared from SPEX's standards stock solutions CLMS-2 and CLMS-4. SPEX's CL-QC-21 was used as a quality control standard. In all samples and standards, indium was used as an internal standard to correct the variation in the signal, for example due to matrix effects.

The dissolution rate for montmorillonite (mol g^{-1} s^{-1}) is calculated from HR-ICP-MS data as described in Rozalen *et al.* (2008), i.e. according to the equation:

$$\mathrm{Rate_{Si}} = -\frac{1}{\nu_{\mathrm{Si}}}\frac{V}{M}\frac{dC_{\mathrm{Si}}}{dt} \quad (1)$$

where ν_{Si} is the stoichiometric coefficient of Si in the dissolution reaction, V is the volume of solution, M is the mass of montmorillonite and dC_{Si}/dt is the slope of the fitted plots. The slope dC_{Si}/dt (see Fig. 5) is selected such that it does not take into account the initial fast dissolution or the stage when the solution has attained saturation with respect to solids as explained in Rozalen *et al.* (2008).

RESULTS

Purification – XRD and SEM analyses

The XRD analysis of the randomly oriented Swy-2 sample indicated that, in addition to smectite, Swy-2 also contains some secondary mineral, such as quartz, K-feldspar and calcite. The oriented samples also showed the presence of kaolinite and some other mineral, which could be identified as mica, illite or interstratified illite/smectite ($I_{>90}$/S). SEM feature analyses of raw Swy-2 revealed secondary minerals, such as quartz, chlorite, plagioclase, biotite, apatite, K-feldspar and calcite. The results of the feature analyses of original Swy-2 are given in Table 2.

The XRD analyses conducted after the purification indicated that quartz and K-feldspar impurities were still present in low amounts. The XRD patterns of the oriented sample indicated the presence of kaolinite as well. The SEM feature analyses showed that most of the secondary minerals had been mainly removed during the

https://doi.org/10.1180/claymin.2013.048.2.11 Published online by Cambridge University Press

TABLE 2. Results of the SEM feature analyses for original Swy-2 (CMS) clay.

Class	% Total features	Feature area (sq. μm)	% Total area
Montmorillonite	86.5	239000	97.66
Quartz	5.8	1880	0.77
K-feldspar	3.6	1280	0.52
Calcite	0.8	357	0.15
Illite	0.7	218	0.09
Plagioclase	0.8	356	0.15
Biotite	0.5	372	0.15
Goethite	0.4	164	0.07
Fe-silicate	0.2	580	0.24
Apatite	0.1	43.2	0.02
Chlorite	0.1	25.2	0.01
Kaolinite	0.1	7.36	<0.01
Fe-oxide	0.1	387	0.16
Grossular	0.1	21	0.01
Monazite	0.1	23.5	0.01

purification process. 99.45% (Table 3) of the material's total area was montmorillonite and the amount of quartz had decreased.

XRD analyses of the test samples

The position of the main smectite peak (001) for raw Swy-2, the purified Swy-2 and the Na-montmorillonite test samples are given in Table 4 for all recorded patterns. In addition to typical smectite peaks, the analyses of Na-montmorillonite samples showed impurities of quartz, K-feldspar and halite. NaCl appeared in Na-montmorillonite samples due to lack of ethanol treatment before the analyses.

The diffraction diagrams of the randomly oriented powders show some variation in (001) peak positions which suggests the presence of different swelling states caused by substitution of the initial interlayer cation Na, totally or partly by the Ca available in the simulant water.

The preparation of oriented samples seemed to blur the differences observed among the randomly oriented samples. The (001) peak position for air-dried oriented samples of all analysed Na-montmorillonites was 12.5 Å±0.2 Å. Swelling clay minerals gave a (001) peak at 17 Å after ethylene-glycol solvation. This smectite peak was observed in all the Na-montmorillonite samples. In the case of fresh water at 25ºC, the ethylene glycol samples

TABLE 3. Results of the SEM feature analyses for purified Swy-2.

Class	% Total features	Feature area (sq. μm)	% Total area
Montmorillonite	93.9	200000	99.45
Goethite	1.9	161	0.08
Quartz	1.9	248	0.12
Kaolinite	0.7	324	0.16
Chlorite	0.4	49.8	0.02
Albite	0.4	64.2	0.03
Calcite	0.4	38.2	0.02
Biotite	0.1	10.1	0.01
K-feldspar	0.1	149	0.07
Illite	0.1	39.8	0.02
Fe-ox	0.1	16.1	0.01

https://doi.org/10.1180/claymin.2013.048.2.11 Published online by Cambridge University Press

TABLE 4. Positions of the (001) peak in measured the XRD patterns of Na-montmorillonite.

Sample Na-montmorillonite	(001) peak positions on randomly oriented powders (in Å)	(001) peak positions on air-dried oriented samples (in Å)	(001) peak positions on ethylene-glycol solvated oriented samples (in Å)
VMV 25ºC	14.7+13.5 (low int)	12.4	17 +13.8
VMV 60ºC	14.5+13.1	12.5	17
VSV 25ºC	14.5	12.6	17
VSV 60ºC	14.7	12.5	17
MV 25ºC	11.26+14.26	12.3	17+13.6
MV 60ºC	11 (low int)	12.4	17
SV 25ºC	14.5	12.4	17
SV 60ºC	14.5	12.4	17
Purified SWY-2 Na-bentonite	11.5	12.5	17
SWY2 (Raw clay)	12.4	12.5	17

VMV = fresh water with solution exchange, VSV = saline water with solution exchange, MV = fresh water, SV = saline water

showed a saddle next to the 17 Å peak (see Table 4), indicating the presence of randomly ordered mixed-layer minerals in addition to smectite. According to Reynolds (1980, 1985), this mineral could be either randomly ordered illite/smectite (I/S = 0) or randomly ordered collapsed (10 Å) smectite/17 Å smectite. Identification of this saddle peak should be completed by additional work.

The major difference between randomly oriented Ca-montmorillonite powders and purified Na Swy-2 and Na-montmorillonites is strongly linked to the interlayer cation (Table 5). The (001) peak of all Ca-smectites is located at 15.0−15.2 Å, which corresponds to two layers of water in the interlayer space. The (001) peak of oriented samples behaves somewhat similarly as in the case of Na-montmorillonite.

When superpositioned (after normalization of intensities of peak 15 Å), the XRD patterns of randomly ordered Ca montmorillonite samples clearly show a deviation in relation to the experimental conditions (Fig. 2). Ca-montmorillonite, in contact with saline water, shows 15 Å peaks less broad than the peak of the reference starting material, whereas the peaks broaden in contact with soft water containing less Ca. The peaks are even broader in the experiments with solution renewal (exchange) than in those without solution renewal.

In the same way, slight displacements and width modifications can be seen on the different peaks of

TABLE 5. Positions of the (001) peak in measured the XRD patterns of Ca-montmorillonite.

Sample Ca-montmorillonite	(001) peak positions of randomly oriented powders (in Å)	(001) peak positions of air-dried oriented samples (in Å)	(001) peak positions of ethylene glycol solvated oriented samples (in Å)
VMV 25ºC	15.1	12.3	17
VMV 60ºC	15.0	12.5	17
VSV 25ºC	15.2	12.6	17
VSV 60ºC	15.1	12.4	17
MV 25ºC	15.2	12.4	17
MV 60ºC	15.1	12.5	17
SV 25ºC	15.1	12.4	17
SV 60ºC	15.1	12.5	17
Purified SWY-2 Ca-bentonite	15.1	12.5	17

https://doi.org/10.1180/claymin.2013.048.2.11 Published online by Cambridge University Press

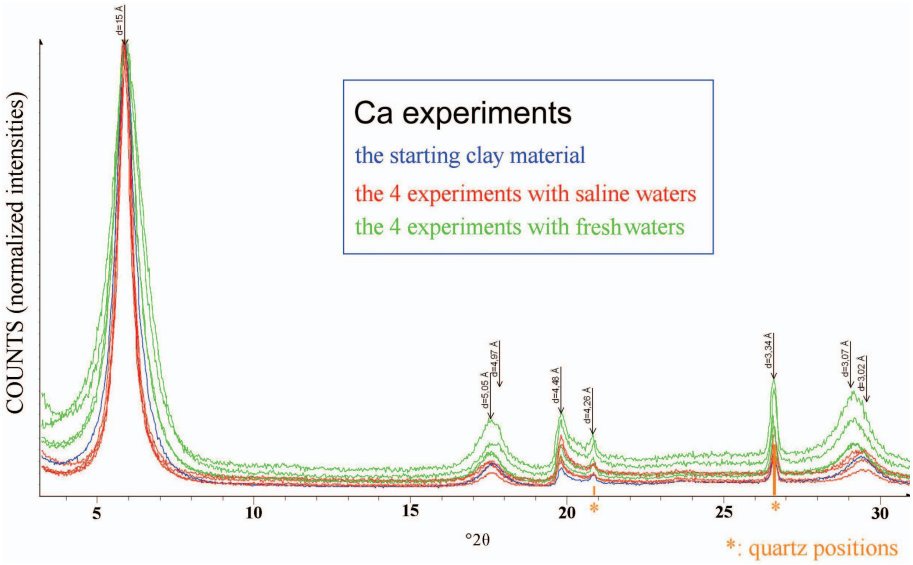

FIG. 2. Superposition (after normalization of the intensities of the 15 Å peak) of XRD patterns recorded in the randomly oriented powders of the nine Ca-samples including the starting material.

the (00l) series. It should be noted that these variations can be seen in the randomly oriented powder diagrams, but not in the oriented sample diagrams because the preparations of the oriented samples makes the patterns more homogeneous.

For the Ca and Na experiments, a set of diagrams (Fig. 3) illustrates theses evolutions for the (001), (003) and (005) peaks which are present in the diagrams (respectively at about 15 Å, 5 Å and 3 Å).

For the Ca experiments (no significant variations of the durations of experiment), the tendencies of separation between VSV (saline waters) and VMV (fresh waters) are marked for the three peaks.

For the Na experiments (with notable variations of the durations of experiments), the evolutions seem to continue with time, but the differences between VSV (saline waters) and VMV (fresh waters) are less obvious. This is because the XRD peaks migrations are more significant than the evolution of the width of the peak.

Comparison of the experimental patterns with the patterns calculated using Newmod (Reynolds, 1985) shows that the experimental patterns are not typical of pure smectites; this is shown by the absence of the (004) reflection (Fig. 4), always present in simulations. To obtain a fit having greater similarities with experimental patterns, the inter-stratification of smectite layers with different thickness is necessary (10, 12−12.5 and 14−15 Å were used). This shows that the material has lost its initial homogeneity and reacts as a complex mixture of interstratified domains, more or less hydrated. This measured behaviour is unstable and seems to be lost when the smectitic material is put in water in order to realize the oriented preparations; it appears as a first step of the transformations and has to be linked to the dissolution phenomena shown by the chemical analyses of the fluids.

HR-ICP-MS analyses

The results of all the elemental analyses are given in a Table 6. The Si concentrations increased as a function of reaction time. At the end of the experiments, the amount of dissolved Si was greatest (~1200 µmol/l) in the saline water at high pH at 60ºC and lowest (~ 80 µmol/l) in the fresh water at 25ºC. The interlayer cation of the starting material had only a minor effect on the amount of dissolved Si in the case of saline waters (Fig. 5). The Si concentrations were slightly elevated in the Ca-montmorillonite tests compared to the tests conducted with Na-montmorillonite.

The Mg concentration stayed mostly under the 2 µmol/l level in the experiments conducted with Na-montmorillonite. In the Ca-montmorillonite experiments the concentration was at the same level in the test with saline water, but notably

https://doi.org/10.1180/claymin.2013.048.2.11 Published online by Cambridge University Press

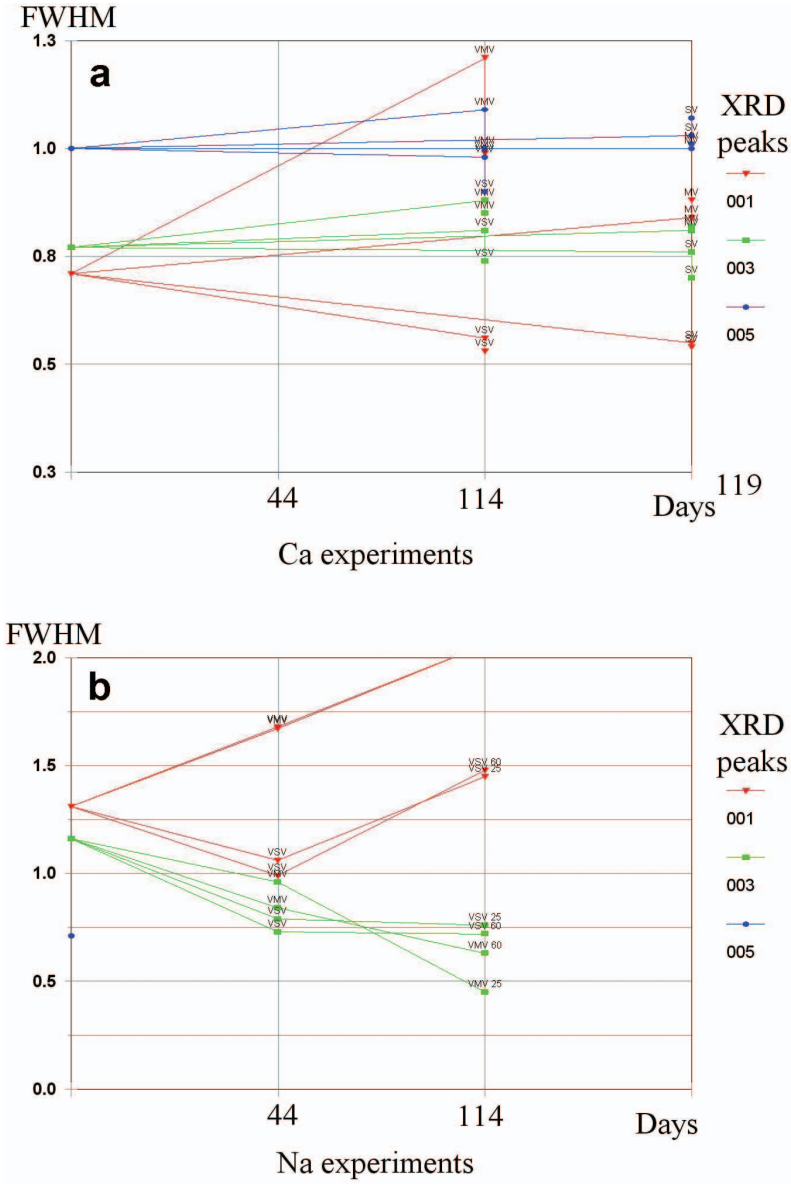

FIG. 3. Evolution of the full width at half maximum intensity (FWHM) for the (00l)peaks of smectite present on XRD patterns recorded on the randomly oriented powders (a: Ca experiments; b: Na experiments).

higher in the fresh water tests at both temperatures. Some trends were also seen in the Mg concentrations. In most cases the initial Mg concentration seemed to decrease, but in the test with Ca-montmorillonite in fresh water the trend of Mg concentration increased throughout the whole experimental time of 140 days.

The Al concentrations were low and Fe concentrations even lower (Table 6). Neither of these concentrations showed any clear trend. The concentrations fluctuated between samplings, which probably was an artefact due to samplings having been performed with ultrafiltration devices. These elements have a high tendency to form precipitates

https://doi.org/10.1180/claymin.2013.048.2.11 Published online by Cambridge University Press

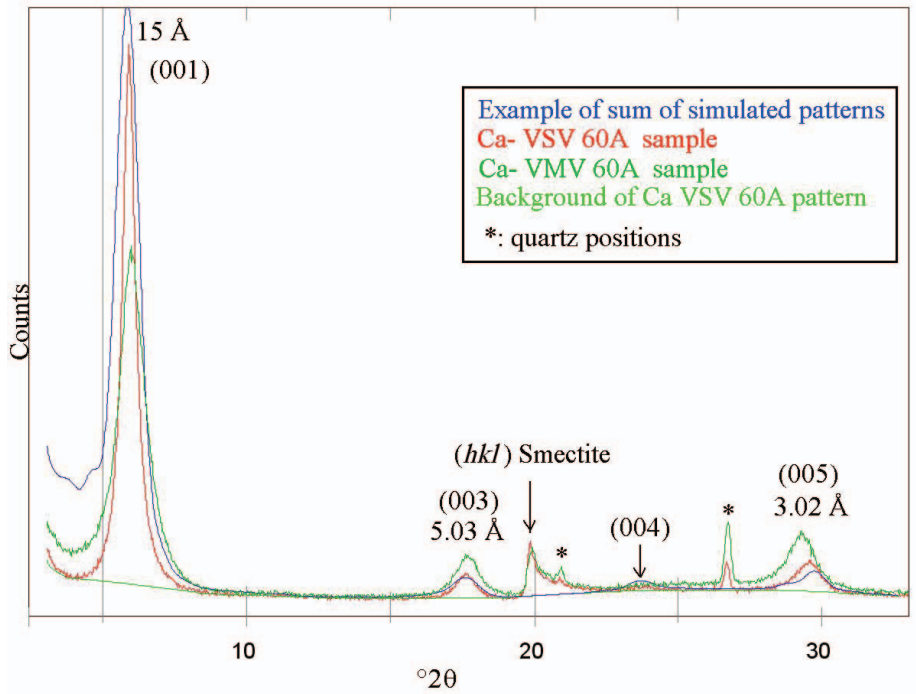

FIG. 4. Representation of XRD patterns recorded of the randomly oriented powders of Ca-VSV60A and Ca-VMV60A samples. The experimental patterns are superimposed with an example of sum of patterns calculated by Newmod (see explanations in text); the simulated patterns are added to the background of the experimental pattern of Ca-VSV60A sample.

and colloids (Rozalen *et al.*, 2008) and thus they could partly be excluded when filtered with as small a pore size of 1 nm.

The Al/Si ratios were calculated to evaluate whether the dissolution was stoichiometric. In all cases the ratio remained under the expected ratio of stoichiometric dissolution.

Rate of dissolution

An indication of smectite dissolution is the amount of dissolved Si, which was used to calculate the dissolution rates. First linear fitting was used for the measured points after the rapid initial dissolution and before the approach of the equilibrium. Thus, the linear fits included the data points from 10 to 40 days, which describe best the stage of sole dissolution. The fitted slopes of Si concentrations are given in Fig. 5. The dissolution rates were obtained from the slopes of linear fits according to equation 1. The logarithmic values of the calculated rates are given in Table 7.

Evolution of pH

The results of the pH measurements are shown in Fig. 6. The initial pH values of 11 and 8 tend to decrease during the experiments as the simulant groundwaters were in contact with the montmorillonite. A slight decrease was observed in most cases considering the whole reaction time. An exception was Na-montmorillonite in contact with fresh water; in those tests the pH first slightly increased and then decreased below the initial pH value of 8. The greatest decrease, over two pH units, was observed in the Na-montmorillonite tests in saline water at 60ºC.

DISCUSSION

The XRD and SEM analyses before and after the purification revealed that the purification procedure was not efficient enough to remove all of the secondary minerals. Small individual grains, under the detection limit of XDR analyses, were identified with SEM, e.g. chlorite or biotite. The SEM images

https://doi.org/10.1180/claymin.2013.048.2.11 Published online by Cambridge University Press

TABLE 6. Analysed elemental concentrations of Mg, Al, Fe and Si (μmol/l) in batch tests during the experiments. The linear fits of dissolution rates (see Figure 5) are based on the bold values.

Specimen	Time (d)	Mg	Al	Fe	Si	Specimen	Time (d)	Mg	Al	Fe	Si
Na MV 25	2	0.98	1.15	0.06	43.9	Ca MV 25	1	1.98	3.13	0.07	36.7
	6	0.32	0.63	0.07	53.4		**4**	2.24	1.20	0.15	**46.2**
	9	0.44	0.73	0.07	**52.4**		**8**	2.25	2.16	0.06	**53.5**
	13	0.38	0.39	0.10	**57.1**		**15**	2.40	1.24	0.05	**55.0**
	17	0.41	0.58	0.12	68.2		22	2.52	0.38	0.06	60.0
	22	0.52	0.44	0.08	66.5		33	2.63	0.54	0.02	63.8
	29	0.45	0.44	0.05	**63.5**		50	2.69	0.04	0.01	65.5
	44	0.43	0.18	0.05	66.5		61	3.19	2.54	0.05	72.0
	56	0.62	0.25	0.04	70.5		80	3.20	1.56	0.07	74.2
	70	0.51	0.32	0.08	66.2		101	3.41	0.93	0.03	78.0
	84	0.57	0.26	0.05	70.5		137	3.30	0.09	0.02	86.8
	105	0.49	0.30	0.05	74.1						
Na SV 25	2	1.98	0.08	0.23	244.0	Ca SV 25	1	1.69	1.17	0.06	178.1
	6	1.74	0.04	0.18	292.3		**4**	1.71	1.88	0.09	**286.4**
	9	1.68	0.49	0.20	**310.5**		**8**	1.66	0.68	0.17	**332.8**
	13	1.61	0.60	0.29	**358.7**		**15**	1.18	1.58	0.11	**379.7**
	17	1.51	0.16	0.24	**370.8**		**22**	0.94	0.76	0.24	**410.7**
	22	1.52	0.64	0.26	372.6		33	0.77	2.95	0.03	521.2
	29	1.18	-0.06	0.01	403.1		50	0.50	0.16	0.03	508.7
	44	0.99	-0.06	0.02	463.5		61	0.76	2.73	0.07	546.9
	56	1.21	0.05	0.03	474.3		80	0.53	1.95	0.05	598.9
	70	1.12	0.04	0.20	495.8		101	0.60	0.77	0.06	671.9
	84	0.89	0.08	0.02	519.6		137	0.44	0.64	0.06	736.1
	105	0.70	-0.04	0.25	567.7						
Na MV 60	1	0.31	0.49	0.07	70.8	Ca MV 60	1	2.47	1.24	0.19	48.5
	5	0.46	1.43	0.16	103.3		4	3.19	2.44	0.05	74.0
	8	0.50	0.70	0.07	106.4		**8**	3.94	2.49	0.39	**95.4**
	12	0.57	0.17	0.06	**125.3**		**15**	4.44	2.52	0.06	**121.9**
	16	0.53	0.26	0.05	**127.8**		**22**	4.92	3.46	0.44	**127.7**
	21	0.66	0.13	0.04	**135.2**		**33**	5.37	2.88	0.13	**142.0**
	26	0.72	0.24	0.04	**152.9**		50	6.06	3.09	0.05	181.2
	36	0.66	0.10	0.03	160.0		61	6.02	1.55	0.04	176.6
	43	0.67	0.12	0.05	162.3		80	6.28	2.43	0.07	198.8
	55	0.92	0.37	0.05	180.8		101	7.80	4.85	0.13	222.8
	69	0.91	0.30	0.04	187.6		137	7.03	1.77	0.03	262.8
	83	0.90	0.09	0.05	196.7						
	104	0.86	0.11	0.11	206.6						
	113				211.4						
Na SV 60	1	1.48	0.11	0.02	201.3	Ca SV 60	1	2.12	2.17	0.08	342.2
	5	0.70	–0.02	0.02	476.5		4	1.06	1.28	0.09	456.1
	8	0.58	–0.05	0.01	539.7		**8**	0.61	0.52	0.25	**620.1**
	12	0.46	–0.10	0.02	**719.6**		**15**	1.10	3.79	0.33	**829.2**
	16	0.43	0.01	0.01	**767.4**		**22**	0.91	1.06	0.11	**916.7**
	21	0.46	0.09	0.01	**870.7**		**33**	0.51	0.44	0.09	**1037.7**
	26	0.47	0.05	0.07	**907.7**		50	0.56	12.01	0.07	1081.4
	36	0.48	0.05	0.03	0.0		61	0.59	1.29	0.06	1165.9
	43	0.54	0.03	0.01	927.1		80	0.81	1.95	0.15	1204.0
	55	0.68	0.05	0.02	872.1		101	0.46	0.53	0.06	1234.0
	69	0.90	0.10	0.03	947.8		137	0.56	0.33	0.05	1231.8
	83	1.23	0.07	0.02	957.1						
	104	7.50	0.05	0.05	988.1						
	113				1046.1						

MV = fresh water, SV = saline water

https://doi.org/10.1180/claymin.2013.048.2.11 Published online by Cambridge University Press

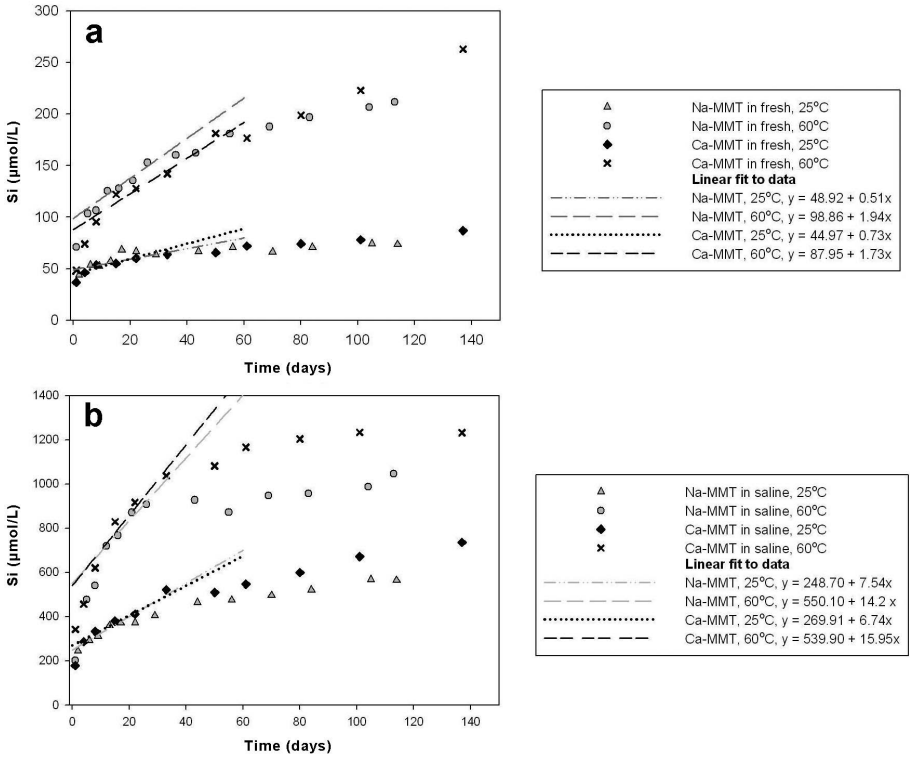

FIG. 5. Evolution of Si concentration during the dissolution of Na- and Ca-montmorillonite in fresh (a) and saline water (b) at 25°C and 60°C.

showed that the amount of secondary minerals decreased greatly during the purification, and the purified material was more homogenous than the raw Swy-2.

In the elemental analyses, the sampling with small pore size filters most probably had an effect on the results for Fe and Al, which tend to form colloids and precipitates as hydroxides and oxides. This was seen as an unsettled fluctuation of the Fe and Al concentrations. This artefact most likely also leads to the result that the Al/Si ratio remained below the expected stoichiometric ratio of 0.38 during the experiments.

The Si and Mg analyses were more successful and showed some observable trends. The interlayer cation did not have a clear effect on the amount of dissolved Si and the dissolution rate, calculated from the release of Si. The dissolution seemed to be

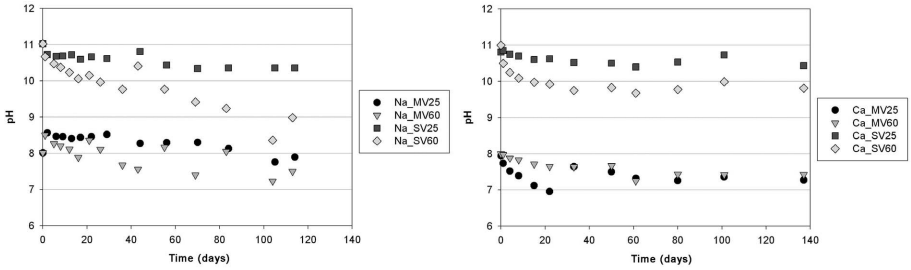

FIG. 6. The evolution of pH in the tests conducted with Na-montmorillonite (left) and with Ca-montmorillonite (right) (MV = fresh water, SV = saline water).

https://doi.org/10.1180/claymin.2013.048.2.11 Published online by Cambridge University Press

TABLE 7. Log rate constants (mol g^{-1} s^{-1}) for Na- and Ca- montmorillonite dissolution.

	Fresh			Saline	
	Na-MMT	Ca-MMT		Na-MMT	Ca-MMT
25ºC, pH 8	–12.13	–11.98	25ºC, pH 11	–11.55	–11.61
60ºC, pH 7.1	–10.96	–11.02	60ºC, pH 10.1	–10.69	–10.64

dependent on the experimental conditions – both water composition and temperature. The elevated temperatures increased the solubility. The higher pH has some increasing effect on reactivity and thus on the solubility, based on the knowledge found in the literature (Lasaga, 1998; Brantley *et al.*, 2008; Rozalen *et al.*, 2008). However, on the basis of the conditions used, it is impossible to say what the role of the salinity in our experiments was. The solubility was increased in saline groundwater simulant with higher pH. In K-montmorillonite dissolution experiments by Zysset & Schindler (1996), the first-order rate constant has been observed to increase with increasing KCl concentration.

As there were trace impurities of quartz in the initial starting material, it should be considered whether the quartz could be the source of dissolved Si and contributes to some small extent to the total Si concentration in the aqueous phase. Brady & Walther (1990) have defined dissolution rates for quartz in comparable pH and temperature conditions to the conditions of the batch experiment conducted in this study. Their dissolution rates indicate that quartz would dissolve at a similar or even slower rate than montmorillonite in our experimental conditions. An exception could be conditions with elevated temperature, 60ºC, and pH 10. In such conditions the dissolution rate of quartz might be slightly higher than that of montmorillonite, causing distortion of total amount of released Si per dissolving mass. The small initial share of, and dissolution rate of quartz, indicate that quartz should not cause a significant effect on the total amount of dissolved Si. The effect on the rate constant (slope of Si release) is even smaller. The estimations based on the pre- and post-experimental XRD analyses of purified Swy-2 agree with such a hypothesis. The estimated proportion of quartz in the analysed materials remains close to the initial proportion or even increases, suggesting that quartz has a similar or slower dissolution rate compared to smectite clay.

The diffraction patterns from randomly oriented Na-montmorillonite samples indicated the substitution of interlayer cation Na by Ca to some extent, but the interlayer space of oriented samples suggested the prevailing interlayer cation to be Na. The analyses of the Na-montmorillonite samples also showed discrepancies regarding the interlayer cation between the randomly oriented and oriented samples. A question of interstratification, observed after some experiments with Na-montmorillonite, remains unsolved. Do the observed changes have any relation with the interstratifications of smectite layers with different hydration states observed by Moore & Hower (1986) in the starting Swy clays, or was it newly created in our experiments?

In terms of X-ray identification, the saturation of smectites with divalent cations (such as calcium) is a useful tool, because it gives a homogenous interlayer composition to the mineral, which produces strong basal reflections at known positions mainly dependent on the analytical conditions (air-dried state or ethylene glycol solvated preparations) (Moore & Reynolds, 1989). Therefore, in the case of Ca samples, heterogeneities like interstratifications of 10 Å dehydrated smectite and hydrated smectite layers cannot be detected, because all the layers exhibit the same behaviour.

However, the superposition of normalized XRD patterns of randomly oriented Ca samples seemed to correlate with the conditions used in the experiments. Among the various parameters, the width of the 15 Å peak is a function of the crystal thickness (or size), i.e. the number of elementary layers stacked in a coherent domain (Brindley, 1980). On the other hand, the peak widening can be a consequence of the increase of disorder in the sample. In these experiments the higher concentration of Ca in saline water decreased the width of the 15 Å peak of the four samples compared to the reference peak of the Ca starting material. This can

https://doi.org/10.1180/claymin.2013.048.2.11 Published online by Cambridge University Press

indicate that the thickness of the smectite material increased or that the ratio of thick particles to thin particles increased, meaning that the dissolution preferred the thinner particles. The experiments realised with fresh waters showed a 15 Å peak broader than the reference starting Ca-montmorillonite. The samples with solution renewal were even wider than the samples without solution renewal. In spite of the fact that the amount of dissolved Si and the rate of dissolution were smaller in fresh solutions, the lower salinity may alter the homogenous interlayer composition of the smectite and induce a decrease of the average size of the coherent domain.

It can be supposed that the heterogeneity of the hydration of smectite layers is a first step in the transformations of the smectite in the conditions of the experiments. Rassineux *et al.* (2001) have studied the alteration of a Wyoming bentonite with more aggressive conditions. The use of complementary data (XRD after Hoffmann-Klemen treatment + additional analyses of the products of the reactions) led to the determination of the modification in the location of the layer charge. It can be imagined that the present works could have led to similar conclusions with more duration in the experiments; the limited transformations are evidenced mainly by the XRD patterns recorded for the randomly oriented powders. Additional work on these samples is necessary to relate these transformations to the location (and to their possible changes) of the charges of the smectite layers.

CONCLUSIONS

The dissolution rates (see Table 5) obtained in our experiments are in agreement with those conducted in aerobic conditions presented in Rozalen *et al.* (2008, 2009) and references therein (Zysset & Schindler, 1996; Bauer & Berger, 1998; Amram & Ganor, 2005; Golubev *et al.*, 2006), even though the pH did not remain stable during the experiments. There were only minor differences in the dissolution rates between Na- and Ca-montmorillonite.

The reactivity increased in saline water with higher pH. To get an idea of the possible effects of the salinity, the experiments in fresh water at pH 11 and the experiments in saline water at pH 8 should at least be conducted in the future.

The results of the XRD and SEM analyses showed that the amount of secondary minerals from the original Swy-2 decreased after the purification. The starting material for the experiments seemed to be quite homogenous, containing a minor amount of quartz. The impurity of quartz has most probably made a small contribution to the amount of dissolved Si. However, the increasing effect of Si, originating from quartz, on the dissolution rate of montmorillonite per mass unit (mol g^{-1} s^{-1}) can be mostly considered as minimal, because of the very similar or even slower dissolution rate of quartz in these conditions. However, in elevated temperature and pH, the effect of quartz impurities on the dissolution rate should be studied more carefully.

The XRD results of the test samples indicated that the 140-day duration running experiments under anaerobic conditions do not produce major mineralogical changes. Regardless of the lack of mineral changes, some modifications of the smectite structures, e.g. in layer stacking can be observed. These can be linked to the dissolution of small amounts of montmorillonite which modify the original stacking.

ACKNOWLEDGMENTS

The research leading to these results has received funding from the Finnish Research Programme on Nuclear Waste Management (KYT) 2011-2014 (BOA project). We acknowledge Kirsti Helosuo, Jaana Rantanen, and Nathalie Bétin for taking part and carrying out their share in the experimental and analytical work. We thank also Marja Siitari-Kauppi (University of Helsinki, Laboratory of Radiochemistry) for her support and creation of collaborative relations during this study.

REFERENCES

Ammann L. (2003) *Cation Exchange and Adsorption on Clays and Clay Minerals.* Dr. rer. nat. dissertation submitted to Faculty of Mathematics and Natural Sciences, Chistian-Albrechts-Universität.

Amram K. & Ganor J. (2005) The combined effect of pH and temperature on smectite dissolution rate under acidic conditions. *Geochimica et Cosmochimica Acta*, **69**, 2535–2546.

Baeyens B. & Bradbury M.H. (1995) A quantitative mechanistic description of Ni, Zn and Ca sorption on Na-montmorillonite. Part I: Physico-chemical characterization and titration measurements. PSI Bericht No. 95-10 and Nagra NTB 95-04, 64.

https://doi.org/10.1180/claymin.2013.048.2.11 Published online by Cambridge University Press

Bauer A. & Berger G. (1998) Kaolinite and smectite dissolution rate in high molar KOH solutions at 35 and 80ºC. *Applied Geochemistry*, **13**, 905–916.

Brady P.V. & Walther J.V. (1990) Kinetics of quartz dissolution at low temperatures, *Chemical Geology*, **82**, 253–264.

Brantley S.L., Kubicki, J.D. & White A.F. (2008) *Kinetics of Water-Rock Interaction.* Springer, New York.

Brindley G.W. (1980) Order-disorder in clay mineral structures. Pp. 125–195 in: *Crystal Structures of Clay Minerals and their X-ray Identification* (G.W. Brindley & G. Brown, editors). Monograph no. 5, Mineralogical Society, London.

Chipera S.J. & Bish D.L. (2001) Baseline studies of the Clay Minerals Society source clays: powder X-ray diffraction analyses. *Clays and Clay Minerals*, **49**, 398–409.

Golubev S.V., Bauer A. & Pokrovsky O.S. (2006) Effect of pH and organic ligands on the kinetics of smectite dissolution at 25ºC. *Geochimica et Cosmochimica Acta* , **70**, 4436–4451.

Knauss K.G. & Wolery T.J. (1987) The dissolution of quartz as a function of pH and time at 70ºC. *Geochimica et Cosmochimica Acta*, **52**, 43–53.

Lasaga A.C. (1998) *Kinetic Theory in the Earth Sciences.* Princeton Series in Geochemistry, Princeton University Press, Princeton.

Malmström M., Banwart S., Lewenhagen J., Duro L. & Bruno J. (1996) The dissolution of biotite and chlorite at 25ºC in the near-neutral pH region. *Journal of Contaminant Hydrology*, **21**, 201–213.

Marty N.C., Cama J., Sato T., Chino D., Villiéras F., Razafitianamaharavo A., Brendlé J., Giffaut E., Soler J. M., Gaucher E.C. & Tournassat C. (2011) Dissolution kinetics of synthetic Na-smectite. An integrated experimental approach, *Geochimica et Cosmochimica Acta*, **75**, 5849–5864.

Moore D.M. & Hower A. (1986) Ordered interstratification of dehydrated and hydrated Na-smectite. *Clays and Clay Minerals*, **34**, 379–384.

Moore D.M. & Reynolds R.C. (1989) *X-ray Diffraction and the Identification and Analysis of Clay Minerals.* Oxford University Press, New York, 332 pp.

Myllykylä E., Tanhua-Tyrkkö M. & Bouchet A. (2011) Alteration and dissolution of Na-montmorillonite in simulated groundwaters. *Materials Research Society Symposium Proceedings*, **1475**, 329–334. Materials Research Society, Buenos Aires, Argentina, 2–7 October 2011.

Rassineux F, Griffault L., Meunier A., Berger G., Petit S., Vieillard P., Zellagui R., & Munoz M. (2001) Expandability-layer stacking relationship during experimental alteration of a Wyoming bentonite in pH 13.5 solutions at 35 and 60ºC. *Clay Minerals*, **35**, 197–210.

Reynolds R.C. (1980) Interstratified clay minerals. Pp. 249–303 in: *Crystal Structures of Clay Minerals and their X-ray Identification* (G.W. Brindley & G. Brown, editors). Monograph 5, Mineralogical Society, London.

Reynolds R.C. (1985) Description of program NEWMOD© for the calculation of the one-dimensional X-ray diffraction patterns of mixed-layered clays. Manuel d'utilisation (R.C Reynolds, editor). 8 Brook Road, Hanover, New Hampsire, 03755.

Rozalen M.L., Huertas F.J., Brady P.V., Cama J., Carcía-Palma S. & Linares J. (2008) Experimental study of the effect of pH on the kinetics of montmorillonite dissolution at 25ºC. *Geochimica et Cosmoschimica Acta*, **72**, 4224-4253.

Rozalen M., Huertas F.J. & Brady P.V. (2009) Experimental study of the effect of pH and temperature on the kinetics of montmorillonite dissolution. *Geochimica et Cosmochimica Acta*, **73**, 3752–3766.

Tournassat C., Greneche J-M., Tisserand D. & Charlet L. (2004) The titration of clay minerals: I. Discontinuous back-titration technique combined with CEC measurements. *Journal of Colloid and Interface Science*, **273**, 224–223.

Wolery T.J. (1992) EQ3NR, A computer program for geochemical aqueous speciation – solubility calculations: theoretical manual, user's guide, and related documentation (Version 7). Lawrence Livermore National Laboratory, Livermore, CA.

Zysset M. & Schindler P.W. (1996) The proton promoted dissolution kinetics of K-montmorillonite. *Geochimica et Cosmochimica Acta*, **60**, 921–931.

https://doi.org/10.1180/claymin.2013.048.2.11 Published online by Cambridge University Press